



Cite this: *Org. Biomol. Chem.*, 2016, **14**, 2504

## Synthesis of inositol phosphate-based competitive antagonists of inositol 1,4,5-trisphosphate receptors†

Vera Konieczny,<sup>a</sup> John. G. Stefanakis,<sup>b</sup> Efstratios D. Sitsanidis,<sup>b</sup> Natalia-Anastasia T. Ioannidou,<sup>b</sup> Nikolaos V. Papadopoulos,<sup>b</sup> Konstantina C. Fylaktakidou,<sup>c</sup> Colin W. Taylor\*<sup>a</sup> and Alexandros E. Koumbis\*<sup>b</sup>

Inositol 1,4,5-trisphosphate receptors (IP<sub>3</sub>Rs) are intracellular Ca<sup>2+</sup> channels that are widely expressed in animal cells, where they mediate the release of Ca<sup>2+</sup> from intracellular stores evoked by extracellular stimuli. A diverse array of synthetic agonists of IP<sub>3</sub>Rs has defined structure–activity relationships, but existing antagonists have severe limitations. We combined analyses of Ca<sup>2+</sup> release with equilibrium competition binding to IP<sub>3</sub>R to show that (1,3,4,6)IP<sub>4</sub> is a full agonist of IP<sub>3</sub>R1 with lower affinity than (1,4,5)IP<sub>3</sub>. Systematic manipulation of this *meso*-compound *via* a versatile synthetic scheme provided a family of dimeric analogs of 2-*O*-butyryl-(1,3,4,6)IP<sub>4</sub> and (1,3,4,5,6)IP<sub>5</sub> that compete with (1,4,5)IP<sub>3</sub> for binding to IP<sub>3</sub>R without evoking Ca<sup>2+</sup> release. These novel analogs are the first inositol phosphate-based competitive antagonists of IP<sub>3</sub>Rs with affinities comparable to that of the only commonly used competitive antagonist, heparin, the utility of which is limited by off-target effects.

Received 21st December 2015,  
Accepted 19th January 2016

DOI: 10.1039/c5ob02623g

www.rsc.org/obc

## Introduction

Inositol 1,4,5-trisphosphate receptors (IP<sub>3</sub>Rs) are intracellular Ca<sup>2+</sup> channels that are almost ubiquitously expressed in animal cells.<sup>1,2</sup> IP<sub>3</sub>Rs are essential links between receptors in the plasma membrane that stimulate phospholipase C and release of Ca<sup>2+</sup> from the endoplasmic reticulum (ER). The resulting cytosolic Ca<sup>2+</sup> signals regulate many diverse cellular processes.<sup>3</sup> The three subtypes of IP<sub>3</sub>Rs expressed in vertebrates (IP<sub>3</sub>R1–3) are closely related proteins and they are each regulated by both (1,4,5)IP<sub>3</sub> (1, Fig. 1) and Ca<sup>2+</sup>, but they differ in their sensitivity to other forms of regulation and in their subcellular and tissue distributions.<sup>1</sup>

Extensive structure–activity studies,<sup>4–8</sup> reinforced by a high-resolution structure of (1,4,5)IP<sub>3</sub> bound to the IP<sub>3</sub>-binding core of IP<sub>3</sub>R1 (Fig. 1A),<sup>9</sup> established that the vicinal 4,5-bisphosphate moiety is essential for (1,4,5)IP<sub>3</sub> binding and the equa-

torial 6-hydroxyl and 1-phosphate confer high affinity (Fig. 1B). All high-affinity agonists of IP<sub>3</sub>R have structures equivalent to these substituents. The only endogenous inositol phosphate likely to bind to IP<sub>3</sub>Rs under physiological conditions is (1,4,5)IP<sub>3</sub>, the immediate water-soluble product of phospholipase C-catalyzed hydrolysis of the membrane lipid phosphatidylinositol 4,5-bisphosphate. However, synthetic ligands of IP<sub>3</sub>Rs, including many inositol phosphates<sup>7</sup> and derivatives of adenophostins,<sup>10–12</sup> have provided insight into the structural determinants of IP<sub>3</sub>R activation. These ligands include analogs of (1,4,5)IP<sub>3</sub> that are resistant to degradation,<sup>13</sup> fluorescent analogs,<sup>14</sup> partial agonists,<sup>6</sup> and synthetic derivatives of adenophostins.<sup>10</sup> There are, however, no ligands of IP<sub>3</sub>R that distinguish effectively between IP<sub>3</sub>R subtypes,<sup>5,15,16</sup> and the only available antagonists have severe limitations.<sup>17</sup> The commonly used antagonists are heparin, 2-aminoethoxydiphenyl borate (2-APB), xestospongins and high concentrations of caffeine. The limitations of these antagonists include off-target effects, notably interactions with other Ca<sup>2+</sup> channels, Ca<sup>2+</sup> pumps, G proteins and other signalling pathways; membrane-impermeability (heparin) and, for xestospongins, an inconsistent history of effectiveness as discussed recently.<sup>17</sup> This study was undertaken with the aim of developing more effective antagonists of IP<sub>3</sub>R.

(1,3,4,6)IP<sub>4</sub>, which retains the essential pharmacophore of an IP<sub>3</sub>R agonist (Fig. 1B), stimulates Ca<sup>2+</sup> release *via* IP<sub>3</sub>R, but its affinity is between 10 and 100-fold lower than that of

<sup>a</sup>Department of Pharmacology, Tennis Court Road, Cambridge, CB2 1PD, UK. E-mail: cwt1000@cam.ac.uk

<sup>b</sup>Laboratory of Organic Chemistry, Chemistry Department, Aristotle University of Thessaloniki, 54124 Thessaloniki, Greece. E-mail: akoumbis@chem.auth.gr

<sup>c</sup>Laboratory of Organic, Bioorganic and Natural Product Chemistry, Molecular Biology and Genetics Department, Democritus University of Thrace, 68100 Alexandroupolis, Greece

†Electronic supplementary information (ESI) available: Synthetic procedures, compound characterization and copies of NMR spectra. See DOI: 10.1039/c5ob02623g



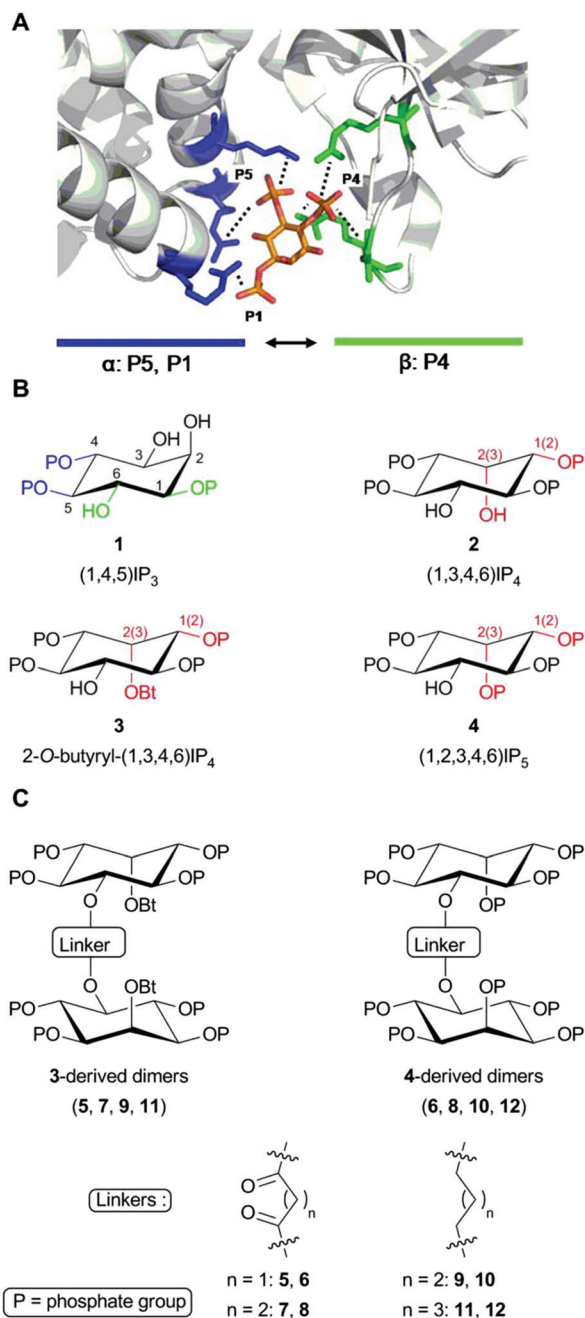


**Fig. 1** Structures of the ligands used. (A) Key contacts between (1,4,5)IP<sub>3</sub> and residues within the IP<sub>3</sub>-binding core (IBC) of IP<sub>3</sub>R1 (Protein Data Bank 1N4K).<sup>9</sup> P4 and P5 form the most extensive interactions (not all are shown) with residues in the β- (in green) and α-domains (in blue) of the IBC, respectively, pulling the two domains towards each other.<sup>23</sup> P1 and the 6-hydroxyl enhance affinity through hydrogen bonding with one residue each within the α-domain. (B) (1,4,5)IP<sub>3</sub> (**1**) showing the essential vicinal (4,5)-bisphosphate (blue) and 6-hydroxyl and 1-phosphate required for high-affinity binding (green). Analogs (**2–4**) are shown in configurations most likely to reflect their interaction with IP<sub>3</sub>R to allow comparison with (1,4,5)IP<sub>3</sub>. Numbers in brackets refer to equivalent groups of (1,4,5)IP<sub>3</sub>. Differences from (1,4,5)IP<sub>3</sub> are highlighted in red. (C) Structures of the dimeric analogs and the acyl or alkyl linkers used.

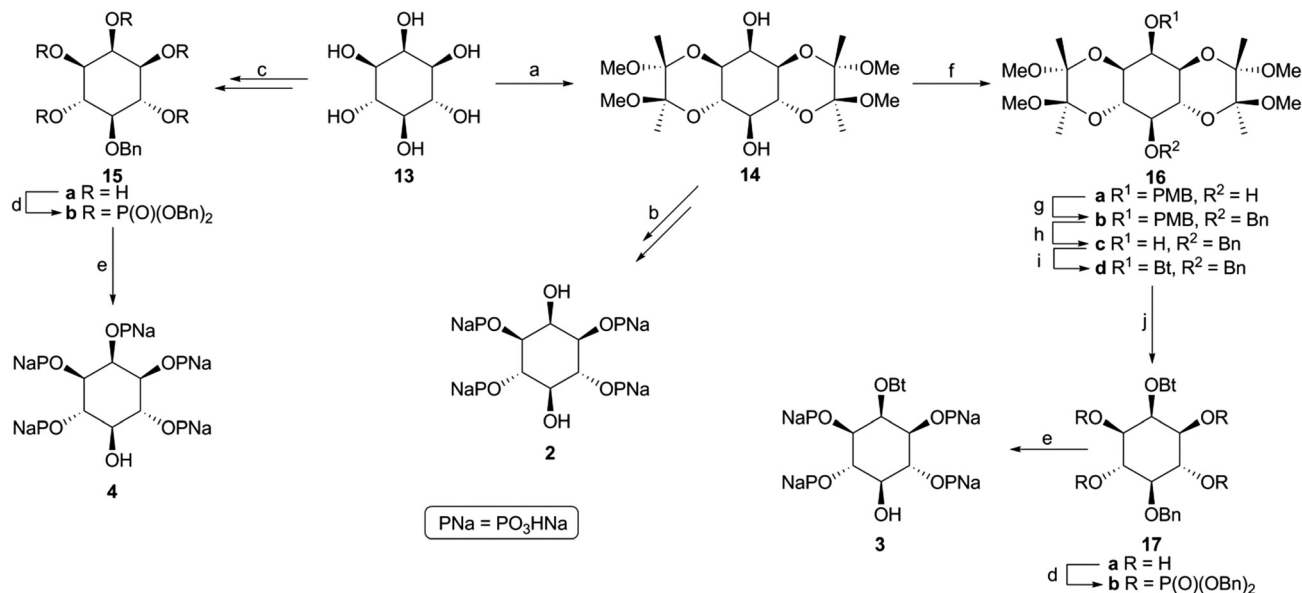
(1,4,5)IP<sub>3</sub>.<sup>18–21</sup> Some,<sup>19,22</sup> though not all,<sup>21</sup> studies have suggested that (1,3,4,6)IP<sub>4</sub> may be a partial agonist, namely that it less effectively activates IP<sub>3</sub>R than full agonists like (1,4,5)IP<sub>3</sub>. It seems likely that the inverted position of the 2-OH in (1,3,4,6)IP<sub>4</sub> (equivalent to the 3-OH of (1,4,5)IP<sub>3</sub> when the structures are compared in orientations likely to reflect their interactions with IP<sub>3</sub>R, Fig. 1B) is a major determinant of the reduced affinity.<sup>5,20</sup> Although (1,3,4,6)IP<sub>4</sub> is produced endogenously from (1,3,4)IP<sub>3</sub>, it is unlikely to attain concentrations that regulate IP<sub>3</sub>Rs.<sup>24</sup> Nevertheless, we chose (1,3,4,6)IP<sub>4</sub> to attempt development of novel antagonists of IP<sub>3</sub>R because it and analogs in which its free hydroxyls are modified (**3**, **4**) are *meso* compounds that make synthesis more straightforward, and we had initially supposed that (1,3,4,6)IP<sub>4</sub> might have reduced efficacy.<sup>19,22</sup> We previously reported that dimers of inositol phosphates are high-affinity partial agonists of IP<sub>3</sub>R.<sup>6</sup> We have now developed a family of antagonists of IP<sub>3</sub>Rs (**5–12** in Fig. 1C) from the (1,3,4,6)IP<sub>4</sub> backbone by modification of its free hydroxyls and dimerization of the modified structures. Diesteric or dietheric linkages of various sizes ( $n = 1–3$ ) were chosen for these 5-*O*-homodimers, which were synthesized by means of a diverse and versatile approach. The most useful of these ligands (**8**, **10** and **12**) bind to IP<sub>3</sub>R1 with an affinity comparable to that of the best available competitive antagonist of IP<sub>3</sub>R, heparin, the utility of which is limited by its off-target effects.

## Results and discussion

### Chemistry

**Synthesis of IP<sub>4</sub>s and IP<sub>5</sub>.** Phosphates **2–4** were all prepared from *myo*-inositol (**13**) (Scheme 1). Thus, tetrasodium (1,3,4,6)IP<sub>4</sub> (**2**) was synthesized from butanedione-derived acetal **14**<sup>25</sup> following a previously published route.<sup>26</sup> Pentasodium (1,2,3,4,6)IP<sub>5</sub> (**4**) was reached *via* pentol **15a** and pentakis phosphate **15b**. Modifications on the perphosphorylation and hydrogenolysis protocols,<sup>26</sup> of an inositol bicyclohexylidene acetal originated synthetic scheme,<sup>27</sup> were applied in order to solely obtain the pentasodium salt. The preparation of butanoate **3** involved a novel approach. Thus, acetal **14** was initially selectively protected at the C-2 position as the PMB ether to yield **16a**. Masking of the remaining C-5 hydroxyl as the benzyl ether gave the fully protected derivative **16b**, which was very carefully deprotected<sup>28</sup> upon treatment with aqueous DDQ to reach free alcohol **16c**. Introduction of the required butyryl group was performed by esterification with butyric anhydride. The resulting ester (**16d**) was then exposed to aqueous TFA to cleave both acetals, and the corresponding tetraol (**17a**) was formed quantitatively. Perphosphorylation of crude **17a** was accomplished using a 1*H*-tetrazole solution in acetonitrile and dibenzyl *N,N*-diisopropylphosphoramidate at ambient temperature, followed by direct oxidation of the intermediate phosphite with *m*-chloroperbenzoic acid at low temperature. Finally, the obtained benzyl tetrakisphosphate **17b** was subjected to hydrogenolysis



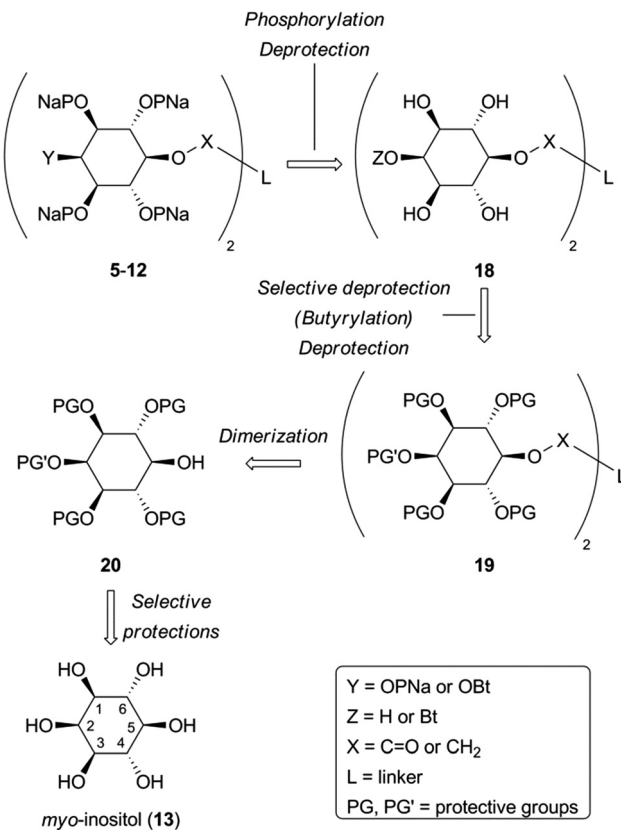


**Scheme 1** Synthesis of phosphates 2–4. Reagents and conditions: (a) ref. 25; (b) ref. 26; (c) ref. 27; (d) i. (BnO)<sub>2</sub>PN(iPr)<sub>2</sub>, 1*H*-tetrazole, CH<sub>3</sub>CN, 25 °C, 48 h; ii. *m*-CPBA, CH<sub>2</sub>Cl<sub>2</sub>, –50 to 0 °C, 5 h, for **15b** 73%, for **17b** 63%; (e) Pd/C, H<sub>2</sub> (1 atm), NaHCO<sub>3</sub>, EtOH/H<sub>2</sub>O (1 : 1), 25 °C, 48–96 h, for **3** and **4** 100%; (f) i. NaH, DMF, 0 °C, 1 h; ii. PMBCl, 0 to 25 °C, 12 h, 67%; (g) i. NaH, DMF, 0 °C, 1 h; ii. BnBr, 0 to 25 °C, 12 h, 90%; (h) DDQ, CH<sub>2</sub>Cl<sub>2</sub>/H<sub>2</sub>O (10 : 1), 25 °C, 24 h, 71%; (i) Bt<sub>2</sub>O, Et<sub>3</sub>N, DMAP, CH<sub>2</sub>Cl<sub>2</sub>, 25 °C, 12 h, 91%; (j) 90% aq. TFA, CH<sub>2</sub>Cl<sub>2</sub>, 25 °C, 2 h, 100%.

in ethanol/water in the presence of Pd/C and sodium bicarbonate (exactly one equivalent per phosphate group) to yield quantitatively the desired tetrasodium salt 3.

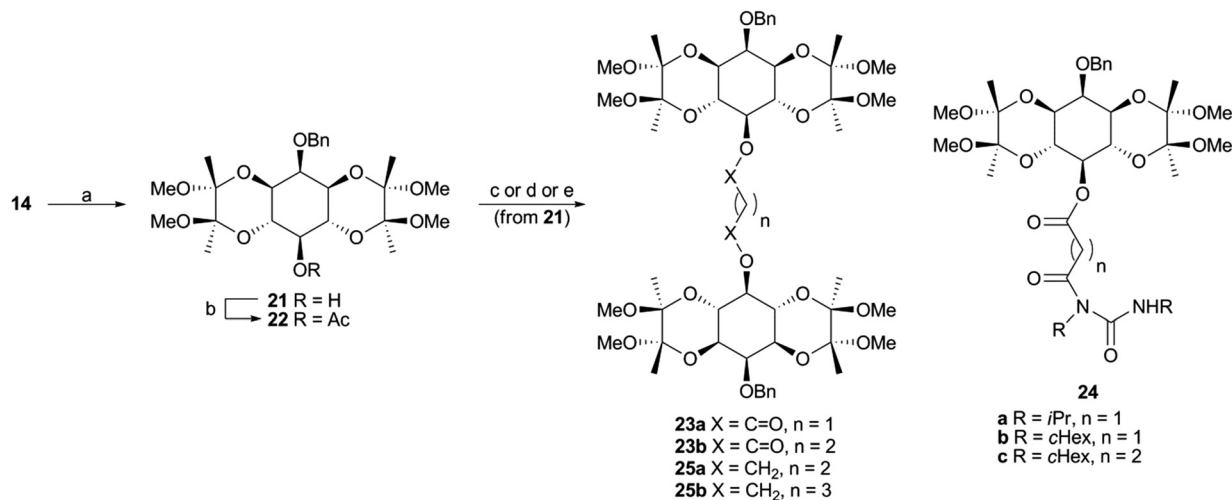
**Synthesis of dimeric analogs of IP<sub>4</sub> and IP<sub>5</sub>.** For the synthesis of dimers 5–12, we envisioned the retrosynthetic analysis depicted in Scheme 2. Dimers 5–12 could be reached from the corresponding polyols **18** applying sequentially perphosphorylation and global deprotection protocols. The key to obtain all these compounds, differentially substituted on C-2, from a common intermediate (**19**) was to introduce orthogonal protective groups (PG and PG') at an early stage of the synthesis. In this way, **19** could serve as the sole precursor for both series (2-*O*-butyrylated and 2-*O*-phosphorylated derivatives) by selective removal of PG'. Esters and ethers **19** could, in turn, be prepared by dimerization of the corresponding monomers **20** using the appropriate linkers. Since this process involved the relatively hindered secondary alcohols **20**, we were keen to explore the feasibility of this approach. Finally, starting from *myo*-inositol (**13**) selective introduction of the required protective groups was expected to lead to monomers **20**.

Monobenzyl ether **21** (Scheme 3) was recognized as a suitable derivative, appropriately functionalized to play the role of **20**. Moreover **21** is easily accessible<sup>25,29,30</sup> from *myo*-inositol through butanedione bisacetal **14**. Direct dimerization of this compound was initially investigated using the Steglich esterification approach<sup>31</sup> and employing malonic ( $n = 1$ ) and succinic acid ( $n = 2$ ) as linkers (Scheme 3 and Table S1 in ESI†). However, these apparently simple couplings were found to be complicated, under various reaction conditions tested, by the formation of acetate **22** (in the first case) and *N*-acylureas **24a–c** (in both cases). Thus, for malonic acid reactions, the presence



**Scheme 2** Retrosynthetic analysis for target dimers 5–12.

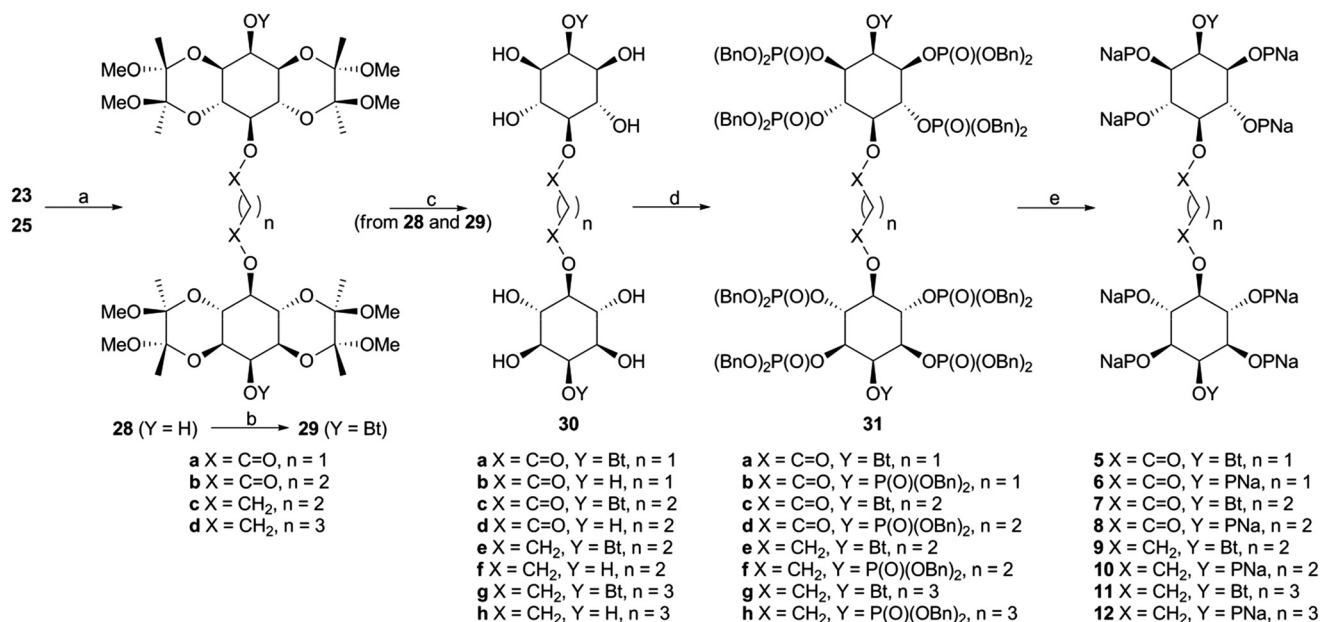




**Scheme 3** Synthesis of dimers **23** and **25**. Reagents and conditions: (a) ref. 29, 30; (b) CH<sub>2</sub>(COOH)<sub>2</sub>, DCC or DIC, DMAP, CH<sub>2</sub>Cl<sub>2</sub>, 25 °C, 24 h, 37–41%; (c) CH<sub>2</sub>(COOH)<sub>2</sub>, DCC, Et<sub>2</sub>O, 25 °C, 24 h, 62% of **23a** and 12% of **24b**; (d) HOCO(CH<sub>2</sub>)<sub>2</sub>COOH, DCC, DMAP, CH<sub>2</sub>Cl<sub>2</sub>, 25 °C, 96 h, 56% of **23b** and 12% of **24c**; (e) TsOCH<sub>2</sub>(CH<sub>2</sub>)<sub>n</sub>CH<sub>2</sub>OTs (**26** or **27**), KOH, BnH/DMSO (4 : 1), 55 °C, 120 h, for **25a** 45%, for **25b** 62%.

of DMAP seemed to solely favor the decarboxylation process, regardless of the carbodiimide (DCC or DIC) and the solvent used.<sup>32</sup> We could not securely determine whether this decarboxylation occurred prior to or after the first esterification. However, in other runs we isolated the *N*-acylureas **24a** and **24b**, suggesting that acetate **22** is formed from malonic monoester. Although replacing DMAP with DIPEA eliminated this problem, the only product isolated was *N*-acylurea **24b**, in very low yield, whereas starting material was quantitatively recovered when EDC was used. On the other hand, the reactions

performed in the absence of base<sup>33</sup> were productive, yielding the desired dimer (**23a**) along with the corresponding *N*-acylurea (**24a** or **24b**). The best results were obtained in the case of the DCC-promoted coupling.<sup>34</sup> Surprisingly, applying the same conditions (DCC in Et<sub>2</sub>O) for the coupling of **21** with succinic acid was unsuccessful. In order to reach dimer **23b** the presence of DMAP was a crucial factor using either DCC or EDC in CH<sub>2</sub>Cl<sub>2</sub>.<sup>34</sup> Again, the reaction with DCC furnished an inseparable mixture of dimer **23b** and *N*-acylurea **24c**, which was subsequently resolved upon hydrolysis. In contrast to



**Scheme 4** Synthesis of dimeric phosphates **5**–**12**. Reagents and conditions: (a) Pd/C, H<sub>2</sub> (1 atm), MeOH, 25 °C, 24 h, 93–100%; (b) Bt<sub>2</sub>O, Et<sub>3</sub>N, DMAP, CH<sub>2</sub>Cl<sub>2</sub>, 25 °C, 24 h, 79–97%; (c) 90% aq. TFA, CH<sub>2</sub>Cl<sub>2</sub>, 25 °C, 2 h, 98–100%; (d) i. (BnO)<sub>2</sub>PN(iPr)<sub>2</sub>, 1*H*-tetrazole, CH<sub>3</sub>CN, 25 °C, 48 h; ii. *m*-CPBA, CH<sub>2</sub>Cl<sub>2</sub>, –50 to 0 °C, 5 h, 60–78%; (e) Pd/C, H<sub>2</sub> (1 atm), NaHCO<sub>3</sub>, EtOH/H<sub>2</sub>O (1 : 1), 25 °C, 48–72 h, 95–100%.



esters **23a,b**, the synthesis of dimeric ethers **25a,b** was accomplished in a more facile way. Williamson etherifications, through the *in situ* formed (NaH) sodium alkoxide of **21**, were initially attempted in DMF using the required diiodo- or dibromo-alkanes, but with poor results. Replacing halo-electrophiles with the more reactive ditosylates **26**<sup>35</sup> and **27**<sup>36</sup> and applying a protocol<sup>37</sup> which involved KOH as base and a more polar solvent (DMSO) furnished the desired dimers (**25a,b**) in a clean way and in good yields.<sup>38</sup>

With the key intermediate dimers in our hands, we proceeded to the next steps, which involved installation of the butyryl and phosphate groups. Pd-catalyzed hydrogenolysis of **23a,b** and **25a,b** led to the corresponding diols **28**, which were esterified upon exposure to butyric anhydride to give **29** in very good yields (Scheme 4).

Both **28** and **29** were then used to reach the final targets. Thus, careful treatment of these dimers (especially in the case of **29**) with aqueous TFA furnished octaols and decaols **30**, in nearly quantitative yields (Scheme 4). Perphosphorylation of these crude polyols was accomplished as described for **17b** (Scheme 1) to obtain the protected polyphosphates **31**. The latter were debenzylated upon hydrogenolysis in the presence of sodium bicarbonate to yield the octakis and decakis phosphate salts **5–12**.<sup>39</sup>

## Biology

**(1,3,4,6)IP<sub>4</sub> is a full agonist of IP<sub>3</sub>R.** Both (1,4,5)IP<sub>3</sub> (**1**) and (1,3,4,6)IP<sub>4</sub> (**2**) stimulated a concentration-dependent release of Ca<sup>2+</sup> from the intracellular stores of permeabilized DT40-IP<sub>3</sub>R1 cells (Fig. 2A and B). The maximal Ca<sup>2+</sup> release evoked by each ligand was similar, but (1,3,4,6)IP<sub>4</sub> was 21 ± 3-fold less potent than (1,4,5)IP<sub>3</sub> (Table S2 in ESI†). Membranes from Sf9 cells expressing rat IP<sub>3</sub>R1 (Sf9-IP<sub>3</sub>R1 cells) were used for equilibrium competition binding studies with <sup>3</sup>H-(1,4,5)IP<sub>3</sub> because these membranes express full-length IP<sub>3</sub>R1 at ~20-fold higher levels than cerebellar membranes, the richest source of endogenous IP<sub>3</sub>R1 (Fig. 2C, inset). In these binding analyses, the equilibrium dissociation constants (*K<sub>d</sub>*) for (1,4,5)IP<sub>3</sub> and (1,3,4,6)IP<sub>4</sub> differed by 46 ± 19-fold (Fig. 2C and Table S2 in ESI†).

Because both agonists (**1** and **2**) released the same amount of Ca<sup>2+</sup> at maximally effective concentrations, a comparison of EC<sub>50</sub> and *K<sub>d</sub>* values allows the effectiveness with which each promotes opening of the IP<sub>3</sub>R Ca<sup>2+</sup> channel to be determined. A partial agonist needs to occupy more receptors to elicit the same response, which is then reflected in a higher EC<sub>50</sub>/*K<sub>d</sub>* ratio (and a lower value for pEC<sub>50</sub>-p*K<sub>d</sub>*, where p denotes the negative log).<sup>6</sup> (1,3,4,6)IP<sub>4</sub> and (1,4,5)IP<sub>3</sub> did not differ significantly in their pEC<sub>50</sub>-p*K<sub>d</sub>* values (Table S2 in ESI†) suggesting that (1,4,5)IP<sub>3</sub> and (1,3,4,6)IP<sub>4</sub> have similar efficacies. We conclude that (1,3,4,6)IP<sub>4</sub> is a full agonist with lower affinity than (1,4,5)IP<sub>3</sub>, in agreement with a previous report,<sup>21</sup> but inconsistent with suggestions that it is a partial agonist.<sup>19,22</sup>

**2-O-Butyryl-(1,3,4,6)IP<sub>4</sub> is a partial agonist and (1,2,3,4,6)IP<sub>5</sub> is an antagonist of IP<sub>3</sub>R.** We synthesized and assessed the biological activity of two analogs with modifications at the 2-position of (1,3,4,6)IP<sub>4</sub>, 2-O-butyryl-(1,3,4,6)IP<sub>4</sub> (**3**) and (1,2,3,4,6)IP<sub>5</sub>

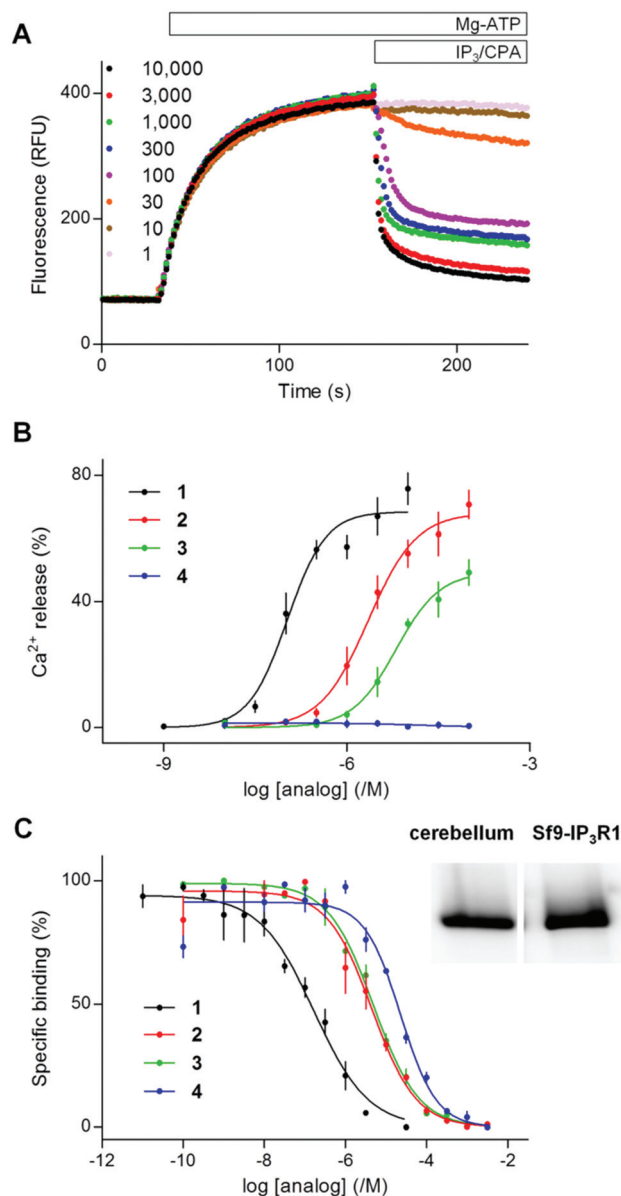


**Fig. 2** 2-O-Butyryl-(1,3,4,6)IP<sub>4</sub> (**3**) is a partial agonist and (1,2,3,4,6)IP<sub>5</sub> (**4**) is an antagonist of IP<sub>3</sub>R. (A) Typical experiment showing Ca<sup>2+</sup> uptake into the ER of permeabilized DT40-IP<sub>3</sub>R1 cells after addition of MgATP (1.5 mM), recorded with a luminal Ca<sup>2+</sup> indicator (mag-fluo4). Addition of (1,4,5)IP<sub>3</sub> (concentrations in nM), with cyclopiazonic acid (CPA, 10 μM) to inhibit the Ca<sup>2+</sup> pump, reveals the concentration-dependent effect of (1,4,5)IP<sub>3</sub> on Ca<sup>2+</sup> release. Results show fluorescence (relative fluorescence units, RFU) as means from triplicate determinations in a single experiment. (B) Summary results show effects of the indicated analogs on Ca<sup>2+</sup> release (% of Ca<sup>2+</sup> content of intracellular stores). (C) Equilibrium competition binding with <sup>3</sup>H-(1,4,5)IP<sub>3</sub> and the indicated analogs using membranes from Sf9-IP<sub>3</sub>R1 cells in CLM containing 1.5 mM MgATP. Results in B and C are means ± s.e.m., *n* = 3. The inset shows a representative Western blot (*n* = 2) demonstrating expression of IP<sub>3</sub>R1 in membranes from rat cerebellum (5 μg protein) and Sf9-IP<sub>3</sub>R1 cells (0.3 μg). Data summarized in ESI in Table S2.†



(4) (Fig. 1B). The analogs retained both the essential pharmacophore (Fig. 1B, blue), and the 5-hydroxyl and 6-phosphate groups [equivalent to the 6-hydroxyl and 1-phosphate of (1,4,5)IP<sub>3</sub>] that increase binding affinity (Fig. 1B, green).

A maximally effective concentration of 2-*O*-butyryl-(1,3,4,6)IP<sub>4</sub> released a smaller fraction of the intracellular Ca<sup>2+</sup> stores than did (1,4,5)IP<sub>3</sub> (Fig. 2B) and it bound to the IP<sub>3</sub>R1 with 50 ± 22-fold lower affinity than (1,4,5)IP<sub>3</sub> (Fig. 2C). The lesser maximal Ca<sup>2+</sup> release evoked by 2-*O*-butyryl-(1,3,4,6)IP<sub>4</sub>, suggests that it is less efficacious than (1,4,5)IP<sub>3</sub>. Although 2-*O*-butyryl-(1,3,4,6)IP<sub>4</sub> and (1,3,4,6)IP<sub>4</sub> differed in their ability to evoke Ca<sup>2+</sup> release, they bound to IP<sub>3</sub>R with similar affinities (Fig. 2C and Table S2 in ESI†). Hence, addition of a butyryl moiety to the 2-position of (1,3,4,6)IP<sub>4</sub> decreased efficacy without affecting affinity. 2-*O*-Butyryl-(1,3,4,6)IP<sub>4</sub> (3) thus replaced (1,3,4,6)IP<sub>4</sub> as a lead compound from which we attempted to develop ligands that bind to IP<sub>3</sub>R without activating it (*i.e.* competitive antagonists).

Even a very high concentration (100 μM) of (1,2,3,4,6)IP<sub>5</sub> (4) failed to release Ca<sup>2+</sup> (Fig. 2B), but it bound to IP<sub>3</sub>R1 with a K<sub>d</sub>

of 22.9 μM (Fig. 2C and Table S2 in ESI†). Hence, (1,2,3,4,6)IP<sub>5</sub> has 230 ± 100-fold lower affinity than (1,4,5)IP<sub>3</sub> for IP<sub>3</sub>R1 and significantly lower affinity than (1,3,4,6)IP<sub>4</sub> or 2-*O*-butyryl-(1,3,4,6)IP<sub>4</sub> (5.2 ± 0.5 and 4.8 ± 0.3-fold lower, respectively) (Fig. 2C, and Table S2, ESI†). (1,2,3,4,6)IP<sub>5</sub> retains the essential pharmacophore and moieties known to be crucial for high-affinity binding (Fig. 1B), but it has an axial phosphate at the 2-position [equivalent to the 3-position of (1,4,5)IP<sub>3</sub>]. Others have reported that an axial phosphate at the 3-position of (1,4,5)IP<sub>3</sub> reduced affinity.<sup>40</sup> The important observation is that addition of an axial 2-phosphate to (1,3,4,6)IP<sub>4</sub>, to give (1,2,3,4,6)IP<sub>5</sub>, abolishes residual efficacy, albeit with some (5.2 ± 0.5-fold) loss of affinity.

Pre-equilibration of permeabilized DT40-IP<sub>3</sub>R1 cells with (1,2,3,4,6)IP<sub>5</sub> (100 μM, 2 min), shifted the sensitivity of the Ca<sup>2+</sup> release evoked by (1,4,5)IP<sub>3</sub> by 2.4 ± 0.2-fold, without affecting either the maximal Ca<sup>2+</sup> release or Hill coefficient (Fig. 3 and Table S3, ESI†). From the dose ratios (see Experimental section), this functional analysis suggests that (1,2,3,4,6)IP<sub>5</sub> binds to the (1,4,5)IP<sub>3</sub>-binding site of IP<sub>3</sub>R1 with a K<sub>d</sub> of ~70 μM. Given the non-equilibrium conditions and the different temperatures used for functional (20 °C) and radioligand binding (4 °C) experiments, this measurement is in reasonable agreement with the affinity determined from equili-

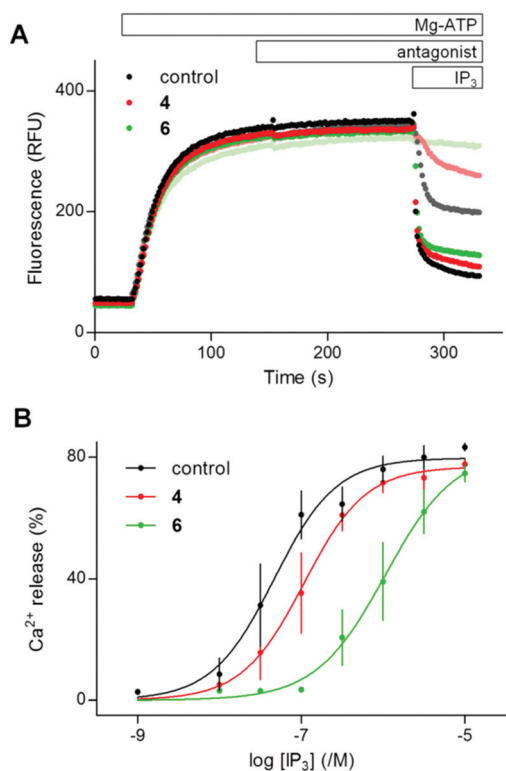


**Fig. 3** (1,2,3,4,6)IP<sub>5</sub> (4) and a dimeric analog (6) are competitive antagonists of IP<sub>3</sub>R1. (A) Typical experiment showing the Ca<sup>2+</sup> content of the ER after addition of Mg-ATP to permeabilized DT40-IP<sub>3</sub>R1 cells, followed by addition of 4 or 6 (100 μM, antagonist) and then cyclopiazonic acid with (1,4,5)IP<sub>3</sub> (100 nM the three upper lighter lines, or 100 μM darker lines). Results show fluorescence as means from 4 repeats within one experiment. (B) Summary shows the concentration-dependent effects of (1,4,5)IP<sub>3</sub> on Ca<sup>2+</sup> release alone or after preincubation with 4 or 6 (100 μM). Results are means ± s.e.m., *n* = 3. Summary results in ESI in Table S3.†

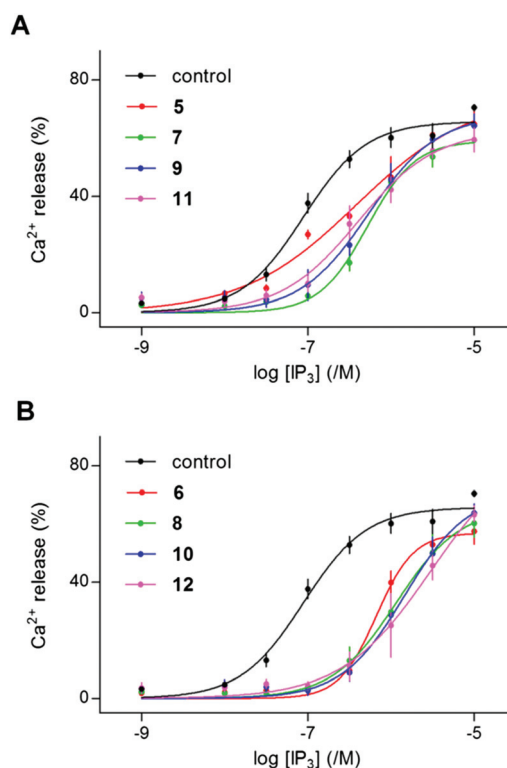


**Fig. 4** Dimers of 2-*O*-butyryl-(1,3,4,6)IP<sub>4</sub> (5, 7, 9, 11) or (1,2,3,4,6)IP<sub>5</sub> (6, 8, 10, 12) are competitive antagonists of IP<sub>3</sub>R1. (A, B) Experiments similar to those shown in Fig. 3 were used to assess the effects of the indicated concentrations of (1,4,5)IP<sub>3</sub> on Ca<sup>2+</sup> release from permeabilized DT40-IP<sub>3</sub>R1 cells after preincubation (2 min) with the indicated dimers (5–12, 100 μM). Results are means ± s.e.m., *n* = 3. Summary results in Table 1.



**Table 1** Dimers of 2-*O*-butyryl-(1,3,4,6)IP<sub>4</sub> and (1,2,3,4,6)IP<sub>5</sub> are competitive antagonists of IP<sub>3</sub>R<sup>a</sup>

	Ca <sup>2+</sup> release					Binding		
	pEC <sub>50</sub> (/M)	ΔpEC <sub>50</sub> (/M)	EC <sub>50</sub> (nM)	Maximal release (%)	n <sub>H</sub>	K <sub>d</sub> (μM)	pK <sub>d</sub> (/M)	K <sub>d</sub> (μM)
(1,4,5)IP <sub>3</sub>	7.03 ± 0.02	—	94	70 ± 1	1.31 ± 0.18	—	6.90 ± 0.19	0.13
+5	6.51 ± 0.06*	0.51 ± 0.03	306	65 ± 6	0.86 ± 0.17	44		
+6	6.03 ± 0.06*	1.00 ± 0.07	931	58 ± 4	1.28 ± 0.08	11	4.79 ± 0.05	16.4
+7	6.14 ± 0.08*	0.89 ± 0.08	719	59 ± 4	1.67 ± 0.57	15		
+8	5.89 ± 0.11*	1.14 ± 0.09	1300	60 ± 5	1.49 ± 0.39	8		
+9	6.24 ± 0.07*	0.79 ± 0.09	571	64 ± 4	1.63 ± 0.42	20		
+10	5.86 ± 0.06*	1.17 ± 0.05	1393	64 ± 3	1.58 ± 0.17	7		
+11	6.27 ± 0.13*	0.76 ± 0.15	537	59 ± 4	1.08 ± 0.17	21		
+12	5.84 ± 0.16*	1.19 ± 0.18	1449	60 ± 5	2.13 ± 0.55	7	5.11 ± 0.08	7.7

<sup>a</sup> Summary results from Fig. 4 show the effects of (1,4,5)IP<sub>3</sub> alone or in the presence of 100 μM of each analog. Results show pEC<sub>50</sub>, ΔpEC<sub>50</sub> (pEC<sub>50</sub><sup>control</sup> - pEC<sub>50</sub><sup>antagonist</sup>) and Hill coefficients (n<sub>H</sub>) (means ± s.e.m.) and EC<sub>50</sub> for (1,4,5)IP<sub>3</sub>-evoked Ca<sup>2+</sup> release (n = 3). K<sub>d</sub> is shown calculated from functional assays and from equilibrium competition binding experiments (n = 3). Statistical differences were determined by one-way ANOVA and Tukey's *post hoc* test, and refer to the results with (1,4,5)IP<sub>3</sub> alone, \*P < 0.05.

rium binding to IP<sub>3</sub>R1 (K<sub>d</sub> ~ 23 μM) (Fig. 2C, 3B and Tables S2, S3 in ESI†). These results demonstrate that (1,2,3,4,6)IP<sub>5</sub> is a competitive antagonist of IP<sub>3</sub>R with an affinity of ~20–70 μM.

**Dimeric analogs of 2-*O*-butyryl-(1,3,4,6)IP<sub>4</sub> or (1,2,3,4,6)IP<sub>5</sub> are antagonists of IP<sub>3</sub>R1 with reasonable affinity.** We reasoned from past precedent<sup>6</sup> that dimeric versions of 2-*O*-butyryl-(1,3,4,6)IP<sub>4</sub> or (1,2,3,4,6)IP<sub>5</sub> might improve affinity or [for 2-*O*-butyryl-(1,3,4,6)IP<sub>4</sub>] the loss of efficacy. We linked 2-*O*-butyryl-(1,3,4,6)IP<sub>4</sub> and (1,2,3,4,6)IP<sub>5</sub> through the 5-*O*-position [analogous to the 6-hydroxyl of (1,4,5)IP<sub>3</sub>] to provide homo-dimeric ligands (5–12, Fig. 1C).

The activities of (1,2,3,4,6)IP<sub>5</sub> (4) and the dimer 6 are directly compared in Fig. 3. Neither 4 nor 6 (100 μM) evoked Ca<sup>2+</sup> release, but they reduced the sensitivity of the Ca<sup>2+</sup> release evoked by (1,4,5)IP<sub>3</sub> by 2.4 ± 0.2 and 20.9 ± 0.7-fold, respectively, without affecting the maximal response or Hill coefficient. Hence the dimer 6, like the monomer 4, is a competitive antagonist, but 6 has an apparent affinity that is 8.8 ± 1.0-fold greater than 4 (Table S3 in ESI†).

The results with 6, suggesting that a dimer of (1,3,4,5,6)IP<sub>5</sub> retained the lack of efficacy of (1,3,4,5,6)IP<sub>5</sub> while displaying improved affinity, prompted analysis of seven additional dimeric analogs of 2-*O*-butyryl-(1,3,4,6)IP<sub>4</sub> and (1,2,3,4,6)IP<sub>5</sub> (Fig. 1C). None of the dimers (5–12, 100 μM) evoked Ca<sup>2+</sup> release, and they all significantly decreased the sensitivity to (1,4,5)IP<sub>3</sub> without affecting the maximal Ca<sup>2+</sup> release or Hill coefficient (Fig. 4 and Table 1). All of the dimers (5–12) are therefore competitive antagonists.

Although 2-*O*-butyryl-(1,3,4,6)IP<sub>4</sub> is a partial agonist with a K<sub>d</sub> of 4.8 μM (Fig. 2B and Table S2 in ESI†), its dimeric analogs are competitive antagonists with slightly reduced apparent affinities (K<sub>d</sub> = 15–44 μM) (Table 1). The decreased affinity is consistent with evidence from analogs of (1,4,5)IP<sub>3</sub>, where substitution of the 6-hydroxyl (equivalent to the 5-hydroxyl of 3, through which the dimers are linked) reduced affinity.<sup>41,42</sup> The 6-hydroxyl of (1,4,5)IP<sub>3</sub> is thought to stabilize interactions of the IP<sub>3</sub>-binding core.<sup>7</sup> However, the reduction in affinity between 3 and its dimers is modest by comparison with the 70

to 100-fold decrease for 6-deoxy-(1,4,5)IP<sub>3</sub> and 6-methoxy-(1,4,5)IP<sub>3</sub> relative to (1,4,5)IP<sub>3</sub>.<sup>41,42</sup> Hence, dimerization of 2-*O*-butyryl-(1,3,4,6)IP<sub>4</sub>, to give 5, 7, 9 and 11, successfully reduced efficacy, but without improving affinity (Table 1).

The antagonist 12 is one of three dimers of (1,2,3,4,6)IP<sub>5</sub> (4) with equally high affinity, and it shifted the EC<sub>50</sub> for (1,4,5)IP<sub>3</sub> by 19.4 ± 6.5-fold, suggesting an apparent K<sub>d</sub> of ~7 μM (Fig. 4B). Given the similar affinities of the dimers 8, 10 and 12 (K<sub>d</sub> 7–8 μM) in functional assays (Table 1), we examined only 12 in equilibrium competition binding experiments. The K<sub>d</sub> value for 12 determined in these experiments (7.7 μM) concurs with the results from functional analyses (Table 1).

These results establish that 8, 10 and 12 are competitive antagonists of IP<sub>3</sub>R with low-micromolar affinity. Although modifications of the 6-hydroxyl of (1,4,5)IP<sub>3</sub> reduced affinity,<sup>41,42</sup> dimerization through the analogous 5-hydroxyls of 3 and 4 caused more modest decreases or increases in affinity, respectively (Table 1). That pattern is similar across the four different linkers used (Fig. 1C). For each linker, dimers of 4 had 2 to 3-fold greater affinity than dimers of 3, even though monomeric 4 has significantly lower affinity than monomeric 3 (Fig. 4, Tables 1 and S2 in ESI†). For dimers of both 3 and 4, the shortest linker (n = 1, Fig. 1C) less effectively increased affinity than did the longer linkers (n = 2–3) (Table 1).

## Conclusions

There is a need for selective antagonists of IP<sub>3</sub>Rs.<sup>17</sup> Aiming to discover new lead-compounds of this type, a series of novel (1,3,4,6)IP<sub>4</sub> and (1,2,3,4,6)IP<sub>5</sub> homodimers were synthesized following a practical synthetic strategy. Among these homodimers, ligands 8, 10 and 12 were the antagonists with greatest affinity for IP<sub>3</sub>R (K<sub>d</sub> 7–8 μM). 5-Carboxymethyl-(1,4)IP<sub>2</sub> was reported to partially inhibit IP<sub>3</sub>-evoked Ca<sup>2+</sup> release, but only at an extremely high concentration (5 mM).<sup>43</sup> (1,3,4,5,6)IP<sub>5</sub> is the only other inositol phosphate previously shown to be a competitive antagonist, but it bound to IP<sub>3</sub>R1 with lower affinity



( $K_d \sim 40 \mu\text{M}$ )<sup>44</sup> than (1,2,3,4,6)IP<sub>5</sub> (**4**,  $K_d \sim 23 \mu\text{M}$ ) and with substantially lower affinity than the dimers of **4**. These comparisons are consistent with our observation that 10  $\mu\text{M}$  (1,2,4,5,6)IP<sub>5</sub> had no detectable effect on (1,4,5)IP<sub>3</sub>-evoked Ca<sup>2+</sup> release,<sup>6</sup> whereas the same concentration of **12** caused a 2.8-fold decrease in (1,4,5)IP<sub>3</sub>-sensitivity (not shown). A dimeric benzene with six attached phosphate groups (biphenyl 2,2',4,4',5,5'-hexakisphosphate) was recently reported to be a rather high-affinity ( $K_d \sim 200 \text{ nM}$ ) antagonist of IP<sub>3</sub>R, but it inhibited IP<sub>3</sub> 5-phosphatase with very similar potency.<sup>45</sup> Compounds **8**, **10** and **12** are the most potent inositol phosphate-based antagonists of IP<sub>3</sub>R so far reported. The affinity of these antagonists for IP<sub>3</sub>R1 ( $K_d$  7–8  $\mu\text{M}$ ) is comparable to that of heparin ( $K_d \sim 4 \mu\text{M}$ ),<sup>17</sup> but the new dimeric antagonists are smaller than heparin ( $M_r \sim 1200$  and  $\sim 5000$ , respectively), and less likely to interact with as many additional intracellular targets. None of these antagonists is membrane-permeant, but based on the versatility of our synthetic approach, it may be feasible to esterify the phosphate groups of the dimeric antagonists to allow them to cross the plasma membrane and then be de-esterified by endogenous intracellular esterases.<sup>46</sup>

## Experimental

### Chemistry

**Materials and methods.** All commercially available reagent-grade chemicals and solvents were used without further purification. Dry solvents were prepared by literature methods and stored over molecular sieves. Whenever possible, reactions were monitored using commercially available precoated TLC plates (layer thickness 0.25 mm) of Kieselgel 60F<sub>254</sub>. Compounds were visualized by use of a UV lamp and/or phosphomolybdic acid (PMA) or Seebach's stains upon warming. Column chromatography was performed in the usual way using Merck 60 (40–60 mm) silica gel using as eluents the solvents indicated in each case. Yields are reported for isolated compounds with >96% purity, as established by NMR spectroscopy. FTIR spectra were obtained in a Nicolet 6700 spectrometer. NMR spectra were recorded with a 300 MHz Bruker Avancelli spectrometer (<sup>1</sup>H: 300 MHz, <sup>13</sup>C: 75 MHz, <sup>31</sup>P: 121 MHz) or an Agilent 500/54 spectrometer (<sup>1</sup>H: 500 MHz, <sup>13</sup>C: 126 MHz, <sup>31</sup>P: 202 MHz) using the deuterated solvent indicated. Chemical shifts are given in parts per million and *J* values in Hertz using solvent or TMS as an internal reference. Assignments of protons were confirmed based on 2D NMR experiments (<sup>1</sup>H, <sup>1</sup>H COSY, HSQC, and HMBC, recorded using a standard pulse-program library). High resolution mass spectra (HRMS) were recorded on microTOF GC-MS QP 5050 Shimadzu single-quadrupole mass spectrometer. For each known compound <sup>1</sup>H and/or <sup>13</sup>C NMR spectra along with HRMS spectra were used to establish identity.

**Esterification of malonic acid with 21.** Malonic acid (280 mg, 2.69 mmol), and DCC (4.43 g, 21.5 mmol) were successively added to a solution of alcohol **21** (2.69 g, 5.39 mmol) in dry Et<sub>2</sub>O (50 mL). The resulting slurry was vigorously stirred

under an Ar atmosphere at room temperature for 24 h, while the reaction progress was monitored by TLC. Upon completion, the solvent was removed *in vacuo*. The residue was triturated with Et<sub>2</sub>O and filtered. The solid was further washed with Et<sub>2</sub>O (25 mL) and the filtrates were concentrated *in vacuo* and the residue was purified with flash column chromatography (hexanes/EtOAc 5 : 1 to 2 : 1) to give 1.78 g (62%) of diester **23a** and 510 mg (12%) of ureido derivative **24b**.

**Esterification of succinic acid with 21.** Succinic acid (160 mg, 1.36 mmol), DMAP (133 mg, 1.1 mmol), and DCC (1.69 g, 8.2 mmol) were successively added to a solution of alcohol **21** (1.36 g, 2.72 mmol) in dry CH<sub>2</sub>Cl<sub>2</sub> (25 mL). The resulting slurry was vigorously stirred under an Ar atmosphere at room temperature for 96 h, while the reaction progress was monitored by TLC. Upon completion, the reaction mixture was washed with H<sub>2</sub>O (25 mL) and saturated brine (25 mL). The combined aqueous phases were back-extracted with CH<sub>2</sub>Cl<sub>2</sub> (4 × 50 mL), the combined organic phases were dried over Na<sub>2</sub>SO<sub>4</sub>, and the solvents were removed *in vacuo*. The residue was purified with flash column chromatography (hexanes/EtOAc 3 : 1 to 1 : 1) to give 820 mg (56%) of diester **23b** and 260 mg (12%) of ureido derivative **24c**.

**General procedure A: preparation of 5,5'-ethers 25a,b.** Alcohol **21** (1 mmol) was dissolved in a 4 : 1 mixture of toluene and DMSO (2.5 mL), powdered KOH (140 mg, 2.5 mmol) was added and the mixture was warmed up to 55 °C. Then, **26**<sup>35</sup> or **27**<sup>36</sup> (0.5 mmol) was added in one portion and the resulting slurry was heated at the same temperature for 120 h, while the progress of the reaction was monitored by TLC. Upon completion, the mixture was neutralized with the addition of a saturated aqueous NH<sub>4</sub>Cl solution. Then, water was added to dissolve all solids and the clear solution was extracted with toluene (50 mL) and CH<sub>2</sub>Cl<sub>2</sub> (2 × 50 mL). The combined organic phases were dried over Na<sub>2</sub>SO<sub>4</sub>, and concentrated *in vacuo*. The residue was purified with flash column chromatography (hexanes/EtOAc 5 : 1 to 1 : 1) to give ethers **25a,b**.

**General procedure B: preparation of diols 28.** 10% Pd/C (200 mg) was added to a solution of dibenzyl ether **23** or **25** (1 mmol) in MeOH (60 mL). This mixture was vigorously stirred under H<sub>2</sub> (1 atm) at room temperature for 24 h. Then, it was filtered through a pad of Celite®, which was further washed with MeOH (20 mL), CH<sub>2</sub>Cl<sub>2</sub> (20 mL), and MeOH (20 mL). Diols **28** were found to be sufficiently pure and used in the next steps without any further purification.

**General procedure C: preparation of butyrates 29.** Dry Et<sub>3</sub>N (0.56 mL, 4 mmol) and DMAP (50 mg, 0.4 mmol) were added to a solution of diol **28** (1 mmol) in dry CH<sub>2</sub>Cl<sub>2</sub> (10 mL) under an Ar atmosphere at room temperature. Butyric anhydride (0.50 mL, 3 mmol) was added and the mixture was stirred at room temperature until the full consumption of starting material (TLC monitoring, about 24 h). The reaction mixture was diluted with CH<sub>2</sub>Cl<sub>2</sub> (20 mL) and successively washed with saturated aqueous sodium bicarbonate solution (3 × 10 mL) and saturated brine (10 mL). The aqueous phase was back-extracted with CH<sub>2</sub>Cl<sub>2</sub> (10 mL) and the combined organic phases were dried over Na<sub>2</sub>SO<sub>4</sub> and concentrated *in vacuo*. The



residue was purified with flash column chromatography (hexanes/EtOAc 7 : 1 to 1 : 1) to give butyrates **29**.

**General procedure D: removal of acetal protecting groups.** A 90% aqueous solution of TFA (10 mL) was added dropwise to a solution of starting acetal (**16d** or **28** or **29**, 1 mmol) in CH<sub>2</sub>Cl<sub>2</sub> (10 mL) at room temperature. The resulting mixture was stirred at the same temperature for 2 h. Then, the volatiles were removed under reduced pressure (40 °C). The residue was successively treated with toluene (10 mL) and absolute EtOH (3 × 10 mL) and each time the solvent was removed under reduced pressure. The resulting polyol was found to be sufficiently pure by NMR and used in the next step without any further purification.

**General procedure E: phosphorylation of polyols.** A 0.45 M solution of 1*H*-tetrazole in CH<sub>3</sub>CN (3 equiv. per OH) was added to a flask containing neat starting polyol (**15a** or **17a** or **30**, 1 mmol) under an Ar atmosphere at room temperature. Then, dibenzyl *N,N*-diisopropylphosphoramidite (1.6 equiv. per OH) was added dropwise over a period of 30 min. The resulting mixture was stirred for 24 h at room temperature, and an additional amount of the phosphorylating agent was added (0.3 equiv. per OH). After 24 h the reaction mixture was diluted with CH<sub>2</sub>Cl<sub>2</sub> (10 mL) and cooled to -50 °C. A solution of 70% *m*-CPBA (2.4 equiv. per OH) in CH<sub>2</sub>Cl<sub>2</sub> (1.6 mL per mmol *m*-CPBA) was added dropwise and the mixture was left to vigorously stir for 5 h at 0 °C. The reaction mixture was further diluted with CH<sub>2</sub>Cl<sub>2</sub> (120 mL) and successively washed with a 10% aqueous solution of sodium sulfite (2 × 150 mL), a saturated aqueous solution of NaHCO<sub>3</sub> (2 × 120 mL), and H<sub>2</sub>O (120 mL). The combined aqueous phases were back-extracted with CH<sub>2</sub>Cl<sub>2</sub> (100 mL). The combined organic phases were washed with saturated brine (120 mL), and dried over Na<sub>2</sub>SO<sub>4</sub>. The solvents were removed under reduced pressure and the residue was purified with flash column chromatography (initially hexanes/EtOAc 2 : 1 to 1 : 2 and then 2–5% CH<sub>3</sub>OH in EtOAc).

**General procedure F: final deprotection.** The starting benzyl phosphate (**15b** or **17b** or **31**, 1 mmol) was dissolved in EtOH (50–70 mL). Deionized H<sub>2</sub>O (50–70 mL) and NaHCO<sub>3</sub> (1 equiv. per phosphate group) were added. Then, 10% Pd/C (1 g) was added to the resulting emulsion and the mixture was vigorously stirred under H<sub>2</sub> (1 atm) at room temperature for the indicating period of time. The reaction progress was monitored by <sup>1</sup>H NMR. Upon completion the catalyst was removed by filtration through an LCR/PTFE hydrophilic membrane (0.5 mm); the membrane was washed with a 1 : 1 mixture of EtOH and deionized H<sub>2</sub>O (3 × 30 mL). The combined filtrates were evaporated under reduced pressure (55 °C), and the resulting residue was dried under high vacuum for 24 h to yield the desired phosphate salt.

## Biology

**Ca<sup>2+</sup> release from permeabilized DT40-IP<sub>3</sub>R1 cells.** DT40 cells with disrupted endogenous IP<sub>3</sub>R genes, and stably expressing rat IP<sub>3</sub>R1 (DT40-IP<sub>3</sub>R1 cells) were cultured as described.<sup>47</sup> For measurements of free [Ca<sup>2+</sup>] within the lumen of the ER,

cells were incubated with mag-fluo4/AM (20 μM, Life Technologies, Paisley, UK) under conditions that favor sequestration of the indicator into the ER lumen.<sup>48</sup> Cells were washed, permeabilized using saponin, resuspended in cytosol-like medium (CLM) supplemented with FCCP [10 μM, carbonyl cyanide 4-(trifluoromethoxy)phenylhydrazone] to inhibit mitochondria, and distributed into black half-area 96-well plates (Greiner Bio-One).<sup>48</sup> CLM had the following composition: 2 mM NaCl, 140 mM KCl, 1 mM EGTA, 20 mM PIPES, 375 μM CaCl<sub>2</sub> (free [Ca<sup>2+</sup>] ~230 nM), pH 7.0. Fluorescence (excitation at 485 nm, emission at 525 nm) was recorded at 1.44 s intervals at 20 °C using a FlexStation 3 plate-reader (MDS Analytical Devices, Berkshire, UK).<sup>48</sup> Ca<sup>2+</sup> uptake into the ER was initiated by addition of 1.5 mM MgATP, and after 2 min (1,4,5)IP<sub>3</sub> or an analog was added with cyclopiazonic acid (CPA, 10 μM, R&D Systems Europe, Oxford, UK) to inhibit further Ca<sup>2+</sup> uptake. Ca<sup>2+</sup> release was recorded after a further 10–20 s and reported as a fraction of the Ca<sup>2+</sup> uptake evoked by ATP. Antagonists were added 2 min before (1,4,5)IP<sub>3</sub>.

**Equilibrium binding of <sup>3</sup>H-(1,4,5)IP<sub>3</sub> and competing ligands to IP<sub>3</sub>R1.** These assays were performed at 4 °C in 500 μL of CLM containing 1.5 mM MgATP, membranes (~20 μg protein) prepared from Sf9 cells expressing rat IP<sub>3</sub>R1 (Sf9-IP<sub>3</sub>R1 cells), <sup>3</sup>H-(1,4,5)IP<sub>3</sub> (1.5 nM, 19.3 Ci per mmol, Perkin Elmer, Waltham, MA, USA) and appropriate concentrations of competing ligand. Non-specific binding was determined by addition of 10 μM (1,4,5)IP<sub>3</sub> (Enzo Life Sciences, Exeter, UK). Reactions were terminated after 5 min by centrifugation (20 000g, 5 min, 4 °C). The pellet was washed with 700 μL of CLM, resuspended in 200 μL of CLM, and radioactivity was determined by liquid scintillation counting. Culture of Sf9 cells, infection with baculovirus encoding rat IP<sub>3</sub>R1, and preparation of membranes were as described previously.<sup>49</sup> Quantification of IP<sub>3</sub>R1 expression by Western blotting, using an anti-peptide antiserum to IP<sub>3</sub>R1<sup>49</sup> was performed as described.<sup>50</sup>

**Analysis.** For each individual experiment, concentration-effect relationships were fitted to a Hill equation using non-linear curve-fitting (GraphPad Prism, version 5). From each experiment, pEC<sub>50</sub> or pIC<sub>50</sub> [-log of the half-maximally effective (EC<sub>50</sub>) or inhibitory (IC<sub>50</sub>) concentration in M], Hill coefficient (*n*<sub>H</sub>), and the maximal response were obtained and then used for statistical analyses. All reported comparisons of ligand potencies rely on comparisons within experiments because EC<sub>50</sub> values for (1,4,5)IP<sub>3</sub>-evoked Ca<sup>2+</sup> release can vary between passages of cells. For convenience, figures illustrating concentration-effect relations show average results from several experiments, but the values (pEC<sub>50</sub>, etc.) determined from fitting curves to individual experiments were used for statistical analyses. Most statistical comparisons were paired, and used Student's *t*-test or one-way ANOVA with Tukey's *post hoc* test as appropriate. *P* < 0.05 is considered significant.

The dose ratio (DR = EC'<sub>50</sub>/EC<sub>50</sub>, where EC'<sub>50</sub> and EC<sub>50</sub> are the EC<sub>50</sub> values for (1,4,5)IP<sub>3</sub>-evoked Ca<sup>2+</sup> release determined in the presence and absence of antagonist, respectively) was used to calculate the apparent affinity (*K*<sub>A</sub>) of IP<sub>3</sub>R1 for



antagonists from functional assays:

$$K_d = \frac{[\text{Antagonist}]}{(\text{DR} - 1)}$$

From equilibrium competition binding experiments, the  $K_d$  of competing ligands was calculated from the concentration ( $\text{IC}_{50}$ ) required to cause 50% displacement of the specifically bound  $^3\text{H}$ -(1,4,5) $\text{IP}_3$ :

$$K_d = \frac{\text{IC}_{50}}{1 + \frac{[^3\text{H}-(1,4,5)\text{IP}_3]}{K_d^{(1,4,5)\text{IP}_3}}}$$

The  $[^3\text{H}-(1,4,5)\text{IP}_3]$  was 1.5 nM, and  $K_d^{(1,4,5)\text{IP}_3}$  (127 nM) (ESI Table S2†).  $\text{p}K_d$  values were then used for statistical analyses.<sup>51</sup>

For comparisons of differences between  $\text{pEC}_{50}$  and  $\text{p}K_d$  values ( $\text{pEC}_{50} - \text{p}K_d$ ), the standard deviation of the difference ( $\sigma_{\text{pEC}_{50} - \text{p}K_d}$ ) was calculated from the individual variances ( $\sigma_{\text{pEC}_{50}}$  and  $\sigma_{\text{p}K_d}$ ):<sup>52</sup>

$$\sigma_{\text{pEC}_{50} - \text{p}K_d} = \sqrt{\sigma_{\text{pEC}_{50}}^2 + \sigma_{\text{p}K_d}^2}$$

## Author contributions

V. K. and J. G. S. contributed equally. A. E. K. initiated the study and supervised the chemistry. C. W. T. designed, interpreted and supervised the biological analyses. V. K. designed, performed and analyzed the biological experiments. J. G. S. and E. D. S. designed the chemical part, performed the synthesis of dimers and interpreted all spectral data. N.-A. T. I. and N. V. P. performed the synthesis of monomers. K. C. F. contributed to formulating the initial rationale. All authors have contributed to the manuscript and approved the final version.

## Abbreviations

Bt	Butyryl
CLM	Cytosol-like medium
<i>m</i> -CPBA	<i>m</i> -Chloro-perbenzoic acid
DCC	<i>N,N</i> -Dicyclohexylcarbodiimide
DDQ	2,3-Dichloro-5,6-dicyano-1,4-benzoquinone
DIC	<i>N,N</i> -Diisopropylcarbodiimide
DMAP	4-Dimethylaminopyridine
$\text{EC}_{50}$ ( $\text{IC}_{50}$ )	Half-maximal effective (inhibitory) concentration
EDC	1-Ethyl-3-(3-dimethylaminopropyl)carbodiimide
ER	Endoplasmic reticulum
$\text{IP}_3$	Inositol trisphosphate
$\text{IP}_3\text{R}$	$\text{IP}_3$ receptor
$\text{IP}_4$	Inositol tetrakisphosphate
$\text{IP}_5$	Inositol pentakisphosphate (structures of the analogs and their codes are shown in Fig. 1)
$K_d$	Equilibrium dissociation constant
$\text{pEC}_{50}$ ( $\text{p}K_d$ )	$-\log \text{EC}_{50}$ ( $K_d$ )

PMB	<i>p</i> -Methoxybenzyl
TFA	Trifluoroacetic acid

## Acknowledgements

Supported by a Senior Investigator Award from the Wellcome Trust 101844 (to C. W. T.), Biotechnology and Biological Sciences Research Council UK and the German Academic Exchange Service (to V. K.). A. E. K. thanks the Research Committee of ATh for financial support. C. W. T. and V. K. thank Dr S. B. Shears (N. I. E. H. S, U. S. A.) for his helpful advice.

## Notes and references

- J. K. Foskett, C. White, K. H. Cheung and D. O. Mak, *Physiol. Rev.*, 2007, **87**, 593.
- C. W. Taylor and S. C. Tovey, *Cold Spring Harbor Perspect. Biol.*, 2010, **2**, a004010.
- M. J. Berridge, M. D. Bootman and H. L. Roderick, *Nat. Rev. Mol. Cell Biol.*, 2003, **4**, 517.
- R. A. Wilcox, W. U. Primrose, S. R. Nahorski and R. A. J. Challiss, *Trends Pharmacol. Sci.*, 1998, **19**, 467.
- E. P. Nerou, A. M. Riley, B. V. L. Potter and C. W. Taylor, *Biochem. J.*, 2001, **355**, 59.
- A. M. Rossi, A. M. Riley, S. C. Tovey, T. Rahman, O. Dellis, E. J. A. Taylor, V. G. Veresov, B. V. L. Potter and C. W. Taylor, *Nat. Chem. Biol.*, 2009, **5**, 631.
- B. V. L. Potter and D. Lampe, *Angew. Chem., Int. Ed. Engl.*, 1995, **34**, 1933.
- A. P. Kozikowski, V. I. Ognyanov, A. H. Fauq, S. R. Nahorski and R. A. Wilcox, *J. Am. Chem. Soc.*, 1993, **115**, 4429.
- I. Bosanac, J.-R. Alattia, T. K. Mal, J. Chan, S. Talarico, F. K. Tong, K. I. Tong, F. Yoshikawa, T. Furuichi, M. Iwai, T. Michikawa, K. Mikoshiba and M. Ikura, *Nature*, 2002, **420**, 696.
- A. M. Rossi, A. M. Riley, B. V. L. Potter and C. W. Taylor, *Curr. Top. Membr.*, 2010, **66**, 209.
- A. M. Vibhute, V. Konieczny, C. W. Taylor and K. M. Sureshan, *Org. Biomol. Chem.*, 2015, **13**, 6698.
- K. M. Sureshan, A. M. Riley, M. P. Thomas, S. C. Tovey, C. W. Taylor and B. V. Potter, *J. Med. Chem.*, 2012, **55**, 1706.
- C. W. Taylor, M. J. Berridge, A. M. Cooke and B. V. L. Potter, *Biochem. J.*, 1989, **259**, 645.
- Z. Ding, A. M. Rossi, A. M. Riley, T. Rahman, B. V. L. Potter and C. W. Taylor, *Mol. Pharmacol.*, 2010, **77**, 995.
- H. Saleem, S. C. Tovey, T. Rahman, A. M. Riley, B. V. L. Potter and C. W. Taylor, *PLoS One*, 2012, **8**, e54877.
- H. Saleem, S. C. Tovey, A. M. Riley, B. V. L. Potter and C. W. Taylor, *PLoS One*, 2013, **8**, e58027.
- H. Saleem, S. C. Tovey, T. F. Molinski and C. W. Taylor, *Br. J. Pharmacol.*, 2014, **171**, 3298.
- I. Ivorra, R. Gigg, R. F. Irvine and I. Parker, *Biochem. J.*, 1991, **273**, 317.
- R. A. Wilcox, S. T. Safrany, D. Lampe, S. J. Mills, S. R. Nahorski and B. V. L. Potter, *Eur. J. Biochem.*, 1994, **223**, 115.



- 20 N. T. Burford, S. R. Nahorski, S.-K. Chung, Y.-T. Chang and R. A. Wilcox, *Cell Calcium*, 1997, **21**, 301.
- 21 P.-J. Lu, D.-M. Gou, W.-R. Shieh and C.-S. Chen, *Biochemistry*, 1994, **33**, 11586.
- 22 D. J. Gawler, B. V. L. Potter, R. Gigg and S. R. Nahorski, *Biochem. J.*, 1991, **276**, 163.
- 23 M.-D. Seo, S. Velamakanni, N. Ishiyama, P. B. Stathopoulos, A. M. Rossi, S. A. Khan, P. Dale, C. Li, J. B. Ames, M. Ikura and C. W. Taylor, *Nature*, 2012, **483**, 108.
- 24 F. S. Menniti, K. G. Oliver, K. Nogimori, J. F. Obie, S. B. Shears and J. W. Putney Jr., *J. Biol. Chem.*, 1990, **265**, 11167.
- 25 S. J. Mills, A. M. Riley, C. Liu, M. F. Mahon and B. V. L. Potter, *Chem. – Eur. J.*, 2003, **9**, 6207.
- 26 A. E. Koumbis, C. D. Duarte, C. Nicolau and J. M. Lehn, *ChemMedChem*, 2011, **6**, 169.
- 27 M. T. Rudolf, T. Kaiser, A. H. Guse, G. W. Mayr and C. Schultz, *Liebigs Ann./Recl.*, 1997, 1861.
- 28 The reaction was closely monitored in order to avoid the oxidative removal of the benzyl group.
- 29 A. M. Riley, H. Wang, J. D. Weaver, S. B. Shears and B. V. L. Potter, *Chem. Commun.*, 2012, **48**, 11292.
- 30 H. Wang, H. Y. Godage, A. M. Riley, J. D. Weaver, S. B. Shears and B. V. L. Potter, *Chem. Biol.*, 2014, **21**, 689.
- 31 B. Neises and W. Steglich, *Angew. Chem., Int. Ed. Engl.*, 1978, **17**, 522.
- 32 We have practically recovered the rest of unreacted starting material (**21**).
- 33 V. V. Mozhaev, C. L. Budde, J. O. Rich, A. Y. Usyatinsky, P. C. Miehels, Y. L. Khmel'nitsky, D. S. Clark and J. S. Dordiek, *Tetrahedron*, 1998, **54**, 3971.
- 34 For large scale runs we have found it more convenient to subject the mixture of **23** and **24** to hydrogenolysis (see Scheme 4), since the debenzylated derivatives were more easily separable.
- 35 A. E. Martin, T. M. Ford and J. E. Bulkowski, *J. Org. Chem.*, 1982, **47**, 412.
- 36 D. H. Bus, D. J. Olszanski, J. C. Stevens, W. P. Schammel, M. Kojima, N. Herron, L. L. Zimmer, K. A. Holter and J. Mocak, *J. Am. Chem. Soc.*, 1981, **103**, 1472.
- 37 P. Goueth, A. Ramiz, G. Ronco, G. Mackenzie and P. Villa, *Carbohydr. Res.*, 1995, **266**, 171.
- 38 Only traces of the corresponding 5-*O*-but-3-enyl- and 5-*O*-pent-4-enyl-derivatives (elimination products) were detected in the reaction mixture.
- 39 For compounds **5** and **6** a rapid H–D exchange of malonic protons in the NMR solvent (D<sub>2</sub>O) occurs. Therefore, these protons disappear in the <sup>1</sup>H NMR spectrum, whereas a quintet is observed in the <sup>13</sup>C NMR spectrum for the CD<sub>2</sub> group (around 40 ppm). The complete insolubility of these compounds in non-protic solvents did not allow us to run other NMR experiments. The provided data (NMR and HRMS) are consisted with the given structures.
- 40 A. P. Kozikowski, V. I. Ognyanov, A. H. Fauq, R. A. Wilcox and S. R. Nahorski, *J. Chem. Soc., Chem. Commun.*, 1994, 599.
- 41 M. A. Polokoff, G. H. Bencen, J. P. Vacca, S. J. DeSolms, S. D. Young and J. R. Huff, *J. Biol. Chem.*, 1988, **63**, 11922.
- 42 S. T. Safrany, R. J. H. Wojcikiewicz, J. Strupish, S. R. Nahorski, D. Dubreuil, J. Cleophax, S. D. Gero and B. V. L. Potter, *FEBS Lett.*, 1991, **278**, 252.
- 43 N. S. Keddie, Y. Ye, T. Aslam, T. Luyten, D. Bello, C. Garnham, G. Bultynck, A. Galione and S. J. Conway, *Chem. Commun.*, 2011, **47**, 242.
- 44 P. J. Lu, W. R. Shieh and C. S. Chen, *Biochem. Biophys. Res. Commun.*, 1996, **220**, 637.
- 45 S. J. Mills, T. Luyten, C. Erneux, J. B. Parys and B. V. L. Potter, *Messenger*, 2012, **1**, 167.
- 46 S. J. Conway and G. J. Miller, *Nat. Prod. Rep.*, 2007, **24**, 687.
- 47 E. Pantazaka and C. W. Taylor, *J. Biol. Chem.*, 2011, **286**, 23378.
- 48 S. C. Tovey, Y. Sun and C. W. Taylor, *Nat. Protocols*, 2006, **1**, 259.
- 49 F. Wolfram, E. Morris and C. W. Taylor, *Biochem. J.*, 2010, **428**, 483.
- 50 S. C. Tovey, S. G. Dedos, E. J. A. Taylor, J. E. Church and C. W. Taylor, *J. Cell Biol.*, 2008, **183**, 297.
- 51 T. P. Kenakin, *A pharmacology primer. Theory, application, and methods*, Elsevier, San Diego, 2004.
- 52 D. Colquhoun, *Lectures in biostatistics*, Clarendon Press, Oxford, 1971.

